Molecular Dynamics Model of Unliganded HIV-1 Reverse Transcriptase

A.T.P. Carvalho, P.A. Fernandes and M.J. Ramos*

Requimte, Departamento de Química, Faculdade de Ciências, Universidade do Porto, Rua do Campo Alegre, 687, 4169-007 Porto, Portugal

Abstract: HIV-1 RT is one of the most important antiviral targets in the treatment of acquired immunodeficiency syndrome (AIDS). Several crystallographic structures are available for this enzyme, mostly with bound inhibitors. Despite their importance for structure based drug design towards new anti-HIV retrovirals, the X-ray structures of the unliganded enzyme could only be obtained incomplete, with a low resolution and until recently even the conformation of the p66 thumb was controversial.

In this work we have aligned different X-ray RT structures, and built up a computational model of RT using homology modeling, which was afterwards refined and validated through MD simulations with explicit solvent.

The model enzyme was structurally stable through the whole MD simulation, showing a RMSD of 2 Å from the starting geometry. The Ramanchandram plot has improved along the simulation. Both intra-domain and interdomain movements were observed. The thumb kept its closed conformation through the whole simulation. A contact map, hydration sites study and a detailed analysis of the solvation of the nucleotide binding site are also presented.

Key Words: HIV-1, Reverse transcriptase, modeling, molecular dynamics.

INTRODUCTION

HIV-1 reverse transcriptase, RT, an essential enzyme for human immunodeficiency virus-1 replication, has distinct catalytic activities that enable it to convert the single stranded RNA of the virus into double-stranded DNA suitable for integration in the host cell genome by HIV-1 integrase [1]. Beyond having a polymerase active site that can copy a RNA and DNA template, HIV-RT has a RNAse catalytic domain that cleaves the RNA strand in the DNA:RNA hybrids and defines the ends of the double stranded DNA.

The enzyme is a heterodimer of 66 and 51 kDa poly-peptides. The two subunits are derived from the gag-pol poly-protein by cleavage by the protease, but p51 lacks the C-terminal domain with the RNAse activity [2].

The subunits share four subdomains that are designed fingers, thumb, palm and connection due to their resemblance to a hand [3]. Although the subunits have the same type of subdomains, the relative subdomain packing is different. p51 which is catalytically inactive is important for the overall reverse transcriptase structure [4].

The fingers, palm and thumb of the p66 subunit form the nucleic acid binding cleft. The palm contains three residues Asp 185, Asp 186 and Asp 110 that are critical for the poly-merase catalytic activity [5, 6].

Due to its key role in HIV-1 infection, the RT enzyme has been subjected to several studies. Kinetic analysis indicated an ordered mechanism, for DNA synthesis by RT, in which primer/template (p/t) binds first followed by addition of dNTP [7]. It was proposed that p/t binding to RT originates two different RT.p/t complexes: a productive com-plex that is capable of nucleotide incorporation, and a non productive complex which has to undergo a conformational change in order to incorporate nucleotides. In addition a dead-end complex incapable of nucleotide incorporation is formed, that can incorporate nucleotide only upon dissoci-ation followed by reassociation [8].

At the same time, X-ray structures for almost all the intermediates in the mechanism of DNA-template based DNA synthesis were determined [9-21]. Furthermore, several structures of RT with bound nucleoside (NRTIs) [20, 21], non-nucleoside inhibitors (NNRTIs) [13, 15, 22-43] and a structure with a DNA-RNA hybrid [44] were also made available.

The superposition of the different crystallographic struc-tures reveals the high degree of flexibility of the enzyme. The most striking difference is the thumb subdomain move-ment that undergoes a 30-40º rigid-body movement relative to the p66 palm subdomain on going from the unliganded enzyme to the E.p/t complex. The conformations are desig-nated closed and open thumb, respectively.

Almost all the crystal structures of the unliganded enzyme display a closed thumb conformation. An open thumb confor-mation is found only in the crystal structure determined by Esnouf *et al.* [11]. However, the structure was produced by soaking out a weak binding non-nucleo-side inhibitor from a pregrown crystal, and hence it cannot be excluded that in this case the open conformation is stabilized by crystal packing.

*Address correspondence to this author at the Departamento de Química, Faculdade de Ciências, Universidade do Porto, Rua do Campo Alegre, 687, 4169-007 Porto, Portugal; E-mail: mjramos@fc.up.pt

1573-4064/06 $50.00+.00 **© 2006 Bentham Science Publishers Ltd.**

Experimental evidence to which conformation was adopted by unliganded RT in solution came from a site directed spin labeling study in which residues Trp24 and Lys287 were replaced by spin-labeled cysteine residues and the distance between them was estimated. The results indicated that unliganded RT adopts primarily the closed thumb conformation at physiological temperatures in solution [45].

In this work we build a new model for RT using "homology modeling". Our model was then subjected to a molecular dynamics simulation with explicit solvent. This new model is excellent for subsequent analysis of the p/t binding to RT a process that is not very well understood yet.

RESULTS

The modeling protocol was different from traditional homology modeling. The templates used were not homologs but different X-ray structures of the same enzyme.

To build the new model for the unliganded HIV-1 RT, (Fig. (**1**)), the highest resolution crystallographic structures were used (listed in the methods section) not only of the unliganded enzyme but also from the enzyme with bound inhibitors.

The binding pocket formed the NNRTIs is located about 10 angstrom away from the polymerase active site and is primarily consisted of residues of the palm and thumb. When the NNRTI burrow and enters the binding pocket it distorts the active site geometry which results in the inability of DNA synthesis to proceed. However, the superposition of unliganded and bound NNRTI enzymatic structures shows differences only in the palm, thumb and fingers [19]. The other domains maintain the same conformation, and hence we could use x-ray structures with bound NNRTIs that have a higher resolution than the available x-ray structures of unliganded RT for these domains.

In this sense the construction of the model was like a puzzle because each domain was built using the highest resolution structure possible for RT.

Because the whole modeling procedure was different some of the quality checks normally used were not applicable. However, the RMS Z-scores for the bond lengths and angles

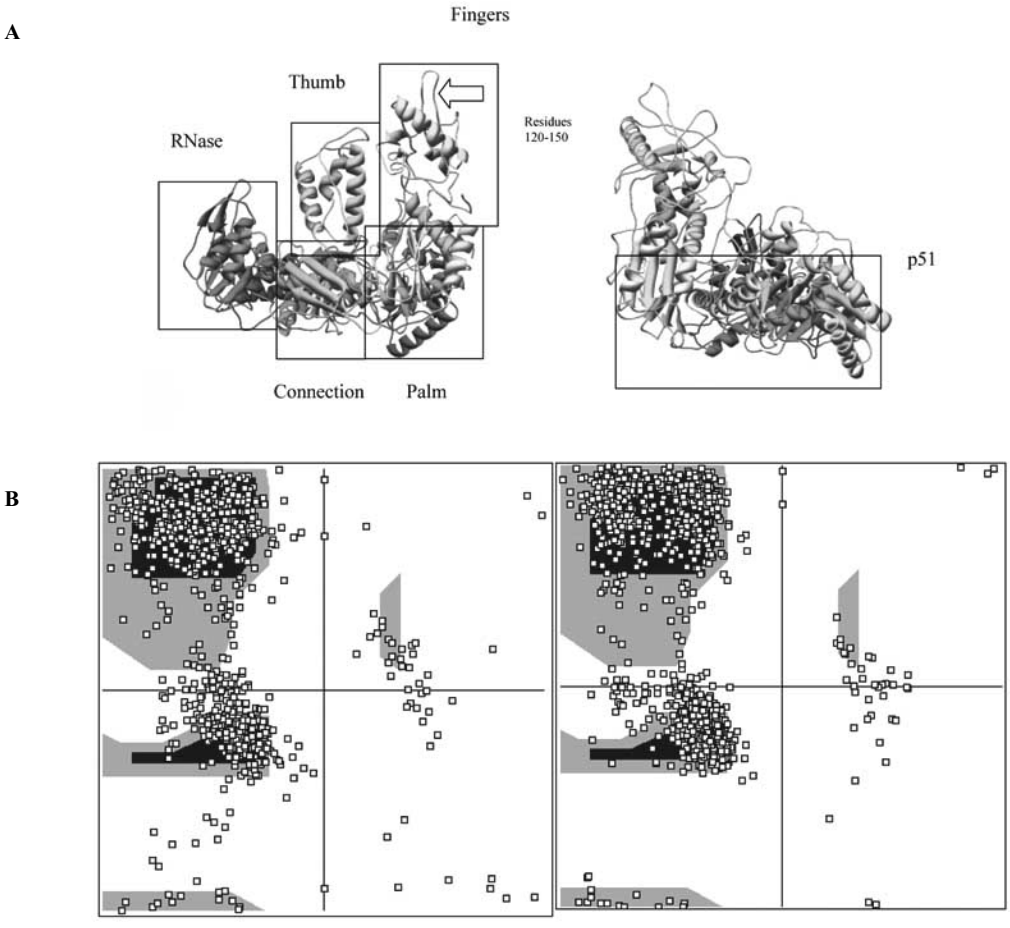

Fig. (1). (A)Two perspectives of the structure of obtained model for unliganded RT. (Left) p66. (Right) p51. (B) Ramanchandran plot for the x-ray structure 1DLO and for the simulated structure.

were 0.813 and 1.098 for p66 and 0.726 and 1.140 for p51 which are good results. The chi1/chi2 rotamer normality Z-score was 4.611 for p66 and 4.177 for p51. The backbone conformation Z-score was -0.245 for p66 and 0.440 for p51. The Ramanchandran plots for the new structure and for the x-ray structure 1DLO are depicted on Fig (**1B**). As can be seen the Ramanchandran plot appearance is better for the new structure.

The structure of unliganded RT is depicted on Fig. (**1A**).

The analysis of the RMS deviation of the Cα carbons along the entire simulation shows that the obtained enzymatic structure is stable and kept the geometry obtained from the modeling process (RMSD ≈ 2). Analyzing the RMS deviation of the two monomers we can see that the p51 structure is kept more rigidly during the course of the simulation, as expected. The p66 subunit has a somewhat larger degree of conformational flexibility Fig. (**2**).

Regarding the domains in the p66 subunit, the RMS deviation of the thumb domain is maintained low during the entire simulation. The region that presents the major value in the RMS deviation from the first structure is the portion of the fingers domain between residues 120 to 150. However, this large variance is not synonymous of thumb-fingers increasing distance, because residues 120-150 are in the extreme opposite from the thumb Fig. (**3**).

Another interesting observation is that the RMSD values for the individual domains are much smaller than the one for the whole p66 subunit, with the exception of the 120-150 region of the fingers domain. This means that the RMSD value for the p66 subunit has a larger contribution from global domain movements, an evidence of both intra and inter domain flexibility.

We begin with a closed thumb conformation structure and, at the end of the simulation the thumb is still in the closed form. The RMSD of the thumb subdomain, as mentioned is maintained low during the whole simulation. Our results are then in agreement with the hypothesis of a closed conformation for unliganded RT, in which, as stated in the literature the p66 subdomain folds down into the DNA binding cleft and makes contacts with the tips of the fingers.

To define the regions of RT that interact with each other in the simulation and specially to analyze the mentioned contacts between thumb and fingers a contact map was calculated. This is shown in Fig. (**4**) along with a map generated from the crystal structure 1DLO for comparison. The new structure maintains the same outline of contacts during the simulation as the crystallographic structure.

The contact maps are similar for the p51 and p66 subunits, except in the region that corresponds to the RNAse domain (residue 438 to 556). The darker spots of the contact map correspond to intradomain close contacts. However, it is also visible some close contacts between the residues of the fingers and thumb with the palm.

Although the thumb is in the closed conformation, there are few contacts between the fingers and thumb during the simulation. The closer contacts between these different

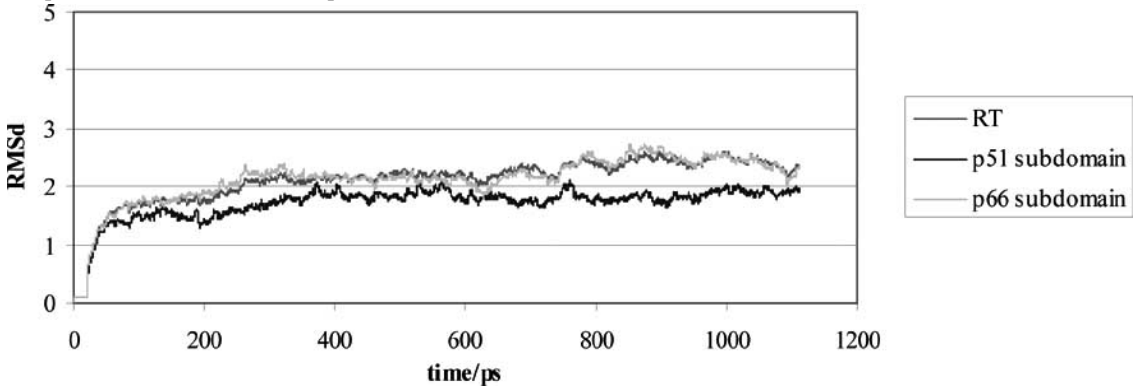

Fig. (2). RMS deviation relative to the first structure of the alpha carbons. The graphic displays the value for the whole enzyme and for the separate monomers.

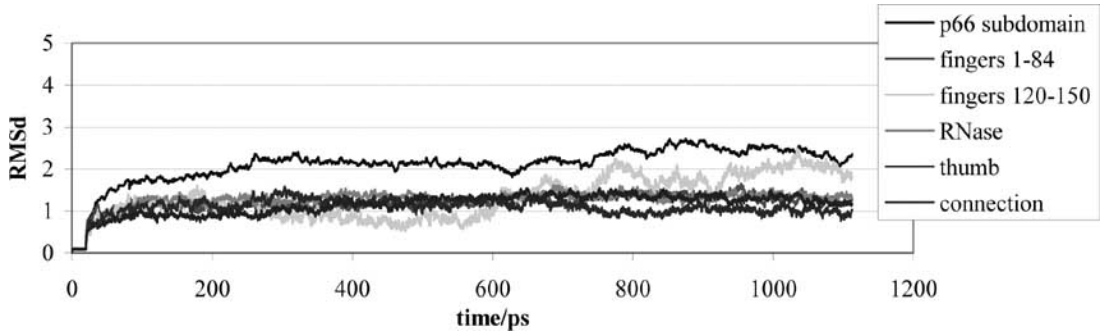

Fig. (3). RMS deviation of the alpha carbons of each p66 subdomain.

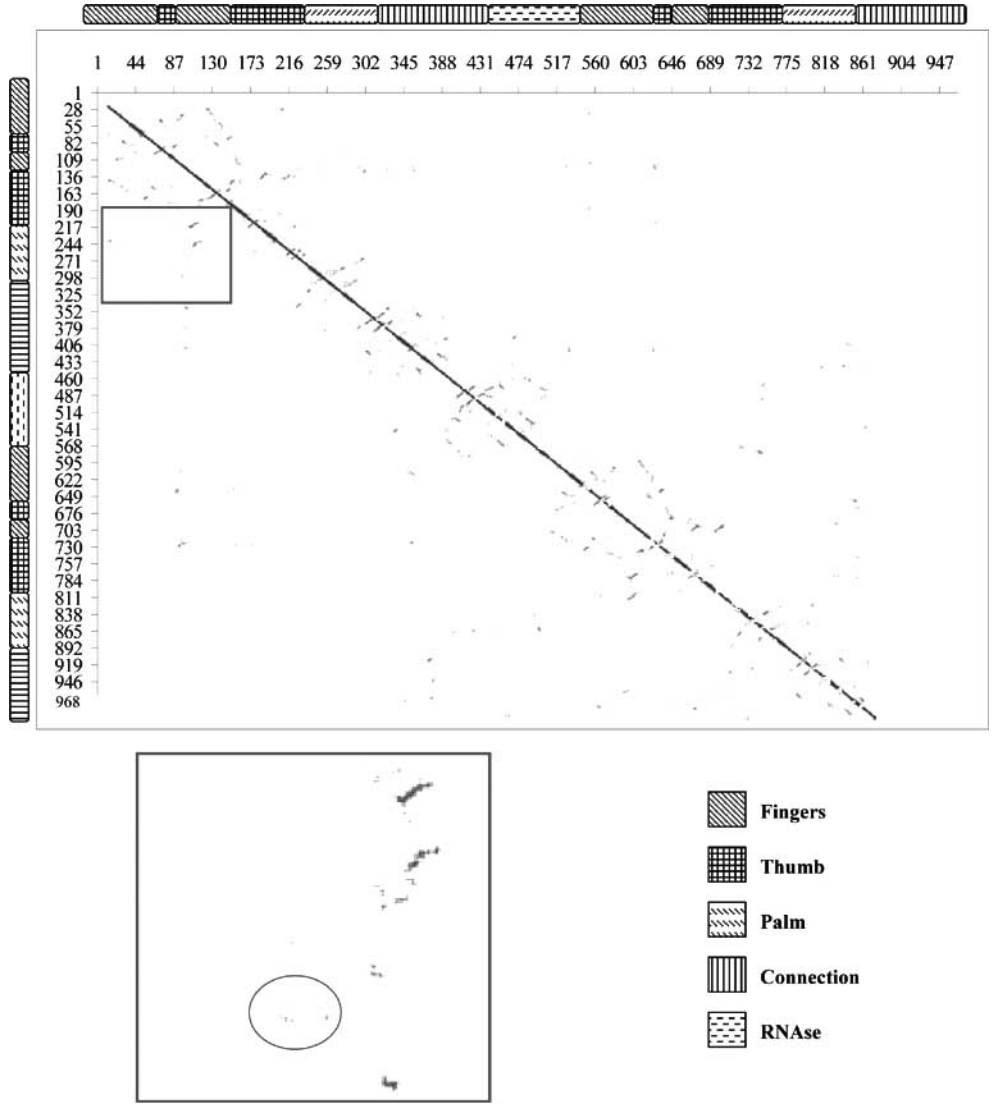

Fig. (4). (A) Cα-Cα Contact maps. (Lower diagonal) Contacts calculated from an average structure obtained from the simulation (from 200 to 1000 ps). (Upper diagonal) Contacts between the alpha carbons of the crystallographic structure 1DLO. A graph square is colored black at 0.0 angstrom distance, to a linear gray scale between 0.0 and 10.0 angstrom and white when equal or greater than 10.0 angstrom.

domains are between 7 and 13 angstrom and hence are not very clear in the contact map, and correspond mainly to combinations of contacts between residues 289 to 290 of the thumb and residues 58-63 and 76, 78 and 79 of the fingers Fig. (**4**).

We measured and plotted the time distance between some of these closer residues. As can be seen in Fig. (**5**) the distances between the alpha carbons of these residues are kept along the simulation, which means that the relative positions of the thumb and fingers domains are kept stable in the closed conformation.

Our results agree with the hypothesis pointed out in the literature that the closed conformation of the thumb subdomain is the preferred state for the unliganded enzyme in solution, as mentioned. However, the time scale for a conformational change such as the thumb movement is larger (should be around 1ns), and hence our simulation time is not enough to exclude the possibility of thumb opening.

In an already mentioned spin labeling study [45], a temperature dependent equilibrium between the open and closed conformations was observed by measuring the distance between residue 24 and residue 287 by EPR, indicating a distinct motion of the thumb subdomain. This hypothetical equilibrium was pointed out to be involved in the translocation of the nucleic acid substrate along the enzyme during polymerization. However, *in vivo*, homeostasis maintains a constant temperature within the cell. Furthermore, the hypothesis of a thumb movement is only applicable during distributive synthesis that is believed to occur only during initiation of DNA synthesis. During polymerization, DNA synthesis is believed to be processive and, in this case, the thumb closing movement should be prevented by steric hindrance with the primer/template.

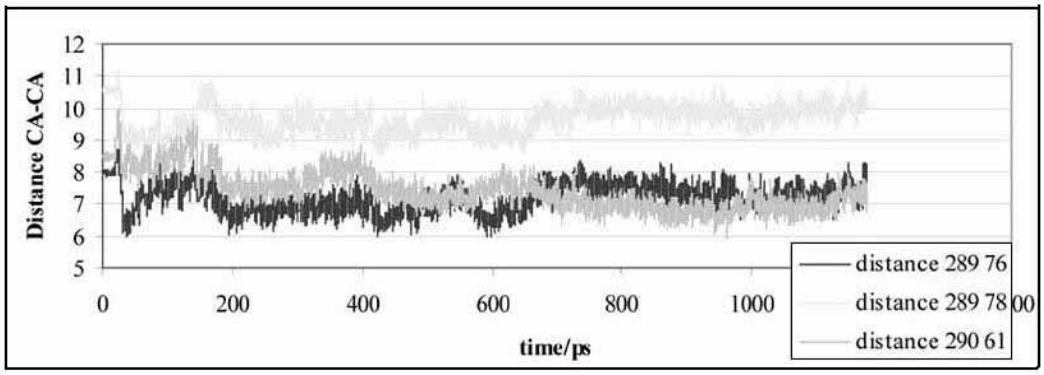

Fig. (5). (A) Cα-Cα distance during the simulation for the residue pairs 289-76, 289-78 and 290 -61. Residues 289 and 290 are located on the thumb tip and 76, 78 and 61 on the fingers.

The dNTP Site

With the determination of the structure of RT with bound p/t and incoming nucleotide came the first description of the dNTP binding site. According to Huang *et al.* the triphosphate moiety of this group is coordinated by Lys65, Arg72, the main chain NH groups of residues 113 and 114 and two metal ions (Mg). One of the Mg ions is coordinated by two oxygens of the pyrophosphate and by a backbone carbonyl (111) and the side chains from aspartates 110 and 185. The 3'OH of the dTTP projects into a small pocket lined by the side chains of Asp113, Tyr 115 Phe 116 and Gln 151 and the peptide backbone between 113 and 115 [19]. The whole binding site is solvated in our model of the unliganded RT.

Interestingly, in our simulated model of unliganded RT the NH group of the residue 113 is involved in a hydrogen bridge with the side chain of Asp185. The Asp110 side chain establishes a hydrogen bridge with Gly112 NH. Finally and regarding the dNTP OH pocket, the side chain of Asp113 establishes a hydrogen bridge with the tyrosine 115 hydroxyl.

These residues are also involved in hydrogen bridges with the solvent. The lifetimes and maximum occupancies are listed on Table **1**.

Therefore, extensive desolvation is needed to the binding of the dNTP. As the substrate is also hydrophobic and charged, a high desolvation penalty should be associated with substrate binding.

However, it is very important to mention that dNTP binding only occurs after primer/template binding. For the p/t to bind, the enzyme has to adopt the open conformation of the thumb. The network of interactions in the bound p/t enzyme is obviously completely different from the unliganded enzyme and then we can not state that the described environment is the same as the one the dNTP encounters.

In order to investigate if the geometry of the binding pocket of the dNTP was maintained within the same accuracy as the rest of the protein during the course of the simulation, we also determined the RMSD profile for these residues. An average RMSD of 2 Å was obtained, showing that a good description of the binding pocket resulted from the computational model.

Table 1. Lifetimes and Maximum Occupancies of Hydrogen Bridges of the dNTP Site Residues with Solvent Molecules

	Lifetime (ps)	Maximum occupancy(ps)
Lys 65 O	8.9	90.2
Arg 72 O	9.3	63
Asp110 OD1	7.2	64.6
Asp110 OD2	7.7	75.8
Asp 110 O	10.0	63
Val 111 O	8.7	63
Gly 112 O	8.3	63
Asp113 OD1	8.8	49.8
Asp113 OD2	8.2	73.8
Asp 113 O	10.5	63
Ala 114 O	8.3	28.4
Phe 116 O	9.8	45.6
Gln151 OE1	6.1	25.8
Gln 151 O	9.9	45.6
Asp185 OD1	8.0	63.0
Asp185 OD2	8.5	163.6
Asp 185 O	11.4	45.6
Asp186 OD1	11.3	127.8
Asp186 OD2	8.9	103.6
Asp 186 O	8.7	27.8

The RMSD for the dNTP site residues during the simulation and in relation to the x-ray structure 1DLO are plotted on Fig. (**6**).

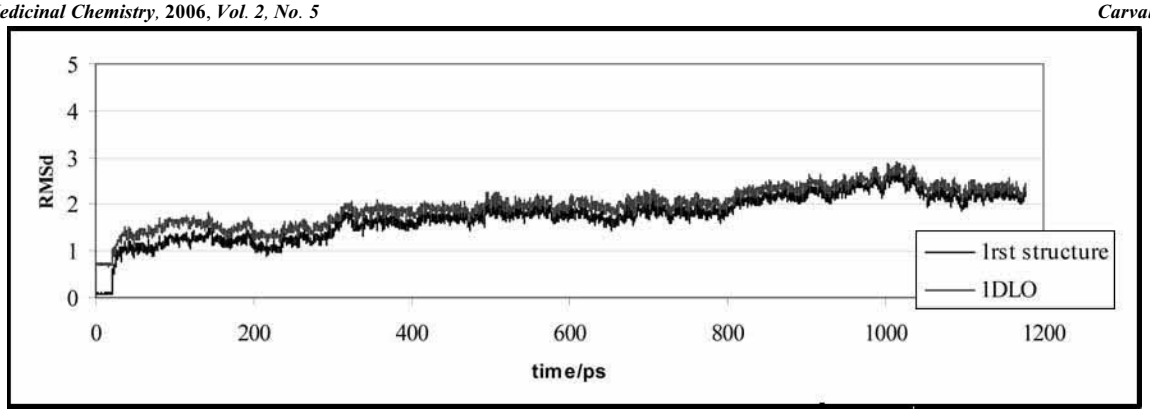

Fig. (6). RMSD for the dNTP site residues during the simulation and in comparison to the X-ray structure 1DLO.

Hydration Sites

The spatial distribution of hydration sites around RT is highly asymmetric and anisotropic around the enzyme (Fig. (**7**)). There are few high-density solvent peaks in the cavity between fingers and thumb and in the connection domains of both subunits. The residues in the areas without high-density solvent peaks do not belong to one particular residue class. In fact, charged and polar residues are found in these regions.

The thumb is positioned in such a way that seems to maximize the interaction of its residues with the solvent in the high-density peaks. This could be one explanation for the apparent higher stability of the closed form in solution.

DISCUSSION

Our obtained model for unliganded RT is an excellent complement to the presently available experimental models of reverse transcriptase. The analysis of the trajectories obtained from the molecular dynamics simulations shows that the structure of the protein is stable. Furthermore, the analysis of the RMS deviations for each subunit and then for each subdomain of the p66 subunit is in agreement with the expected. All values are small, typically between 1-2 ansgtrom and the p66 subunit presents a larger degree of flexibility relative to p51.

In the p66 subunit the portion of the finger tips between residues 120 to 150 presents the larger degree of flexibility. The RMS deviation of the alpha carbons of the thumb is relatively low (below 1.5 Å).

The new structures establish close contacts mainly between residues of the same domain. However some close contacts between the thumb and palm and between the fingers and palm are also observable in the contact map. Interestingly, the fingers and thumb, in the closed form, establish few contacts. Following the distance over time of these close contacts between the two domains we can see that the distance between them stabilizes, which is indicative of the stability of the closed form of unliganded RT.

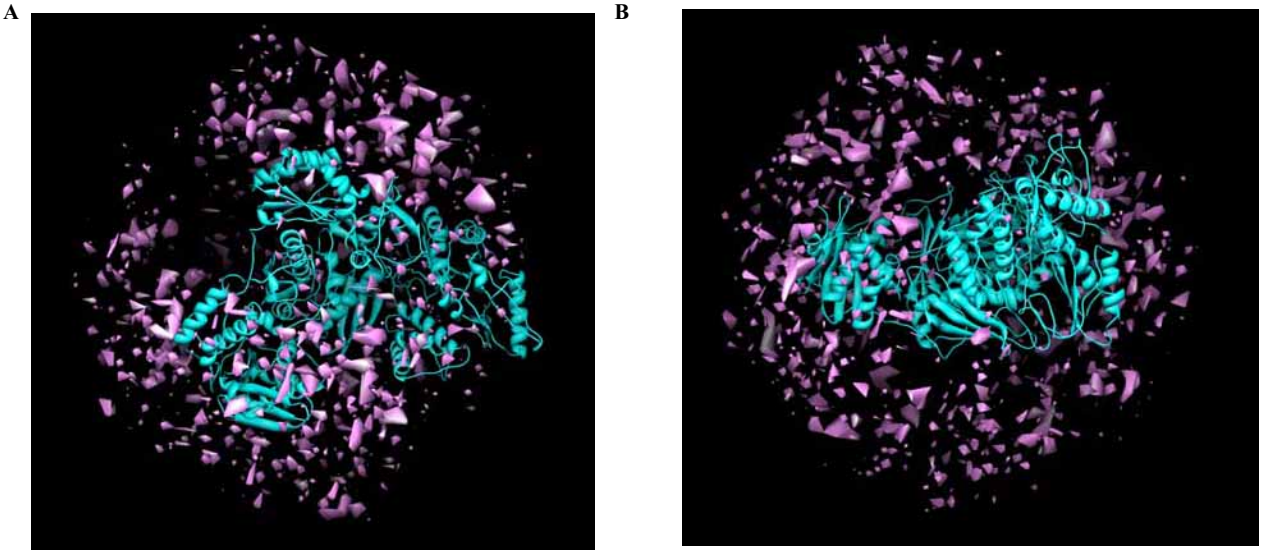

Fig. (7). Three-dimensional distribution of high-density solvent peaks around RT. The figures correspond to two different orientations of the same enzyme.

The solvation of the dNTP binding site was also studied. It was shown that this site is extensively solvated in the unliganded state. Almost all the binding site residues are accessible to the solvent. The hydrogen bonding network with the solvent and the mean and maximum lifetime of the hydrogen bonds with the solvent were also analyzed. The RMSD between the 1DLO crystallographic structure and the computational model exhibit a value around 2 Å during the whole simulation.

Observing the three dimensional distribution of high density peaks around RT, it seems that the thumb is positioned in such a way that maximizes the interaction of its residues with the solvent in these high density peaks. This could be a factor that could explain the stability of the closed form of RT. However, longer simulation runs are necessary to assure that the closed conformation of the thumb is the preferred one in solution.

METHODS

Modeling

The structure of HIV-1 RT was obtained by performing a multiple sequence alignment of domains of the available x-ray structures. For the p66 subunit the following crystallographic structures were used: the p66 subunit of the unliganded RT 1DLO (2.70 Å resolution) [12] the p66 subunit of the mutated unliganded enzyme 1QE1 (2.85 Å resolution) [14], the connection domain of structure 1RTJ (2.35 Å resolution) [11] and the RNAse domain of 1RTH (2.2 Å resolution) [26] (Fig. (**6**)).

For the most rigid p51 subunit we used the p51 subunit of 1RTJ [11], the 51 kDa polypeptide of the complex rt-U05 1RTH [26] and the p51 subunit of the complex rt-nevapirine 1VTR (2.2 Å resolution) [26].

As previously stated, our choice of the structures used for templates was based in the known rigidity of some domains. The best resolution structures of RT are bound to NNRTIs or are derived from crystals grown in the presence of an NNRTI. It is known by superposing the determined x-ray structures that some domains of RT have the same conformation in the presence of the inhibitor as in the unliganded state (connection and RNAse of p66 and p51 subunit). We used only the connection domains of 1RTJ because, although this structure has one of the best resolutions for unliganded RT, it presents the thumb in the open form as a result of soaking an NNRTI from a pregrown crystal. The 1RTH and 1VTR x-ray structures are complexed with NNRTI inhibitors, so we used them as templates only for the p51 subunit.

This was again verified by superimposing the structures (data not shown).

The performed alignments for each subunit were then submitted to Swiss model protein structure homology modeling server [46]. It is worth mention that the entire templates used were from the same enzyme and hence the obtained structure is more reliable than one obtained from a normal homology modeling procedure. The quality of the models was verified using the WHAT IF program [47].

The obtained theoretical models for each subunit were then merged to form the heterodimer.

Molecular Dynamics

The energy minimizations and molecular dynamics simulations were carried using the SANDER module of the amber 8 package [48]. We began by adding the missing hydrogens using the LEAP module. Subsequently, eight Cl- ions were added to neutralize the system. The structure was then solvated with an octahedral box of TIP3P waters with each box side at a distance of at least 15 Å from the protein (180278 waters).

The minimizations were then performed with the parm94 force field [49]. Firstly, we equilibrated the solvent and ions maintaining the protein atoms constrained by weak harmonic restraints. Then we performed 1500 steps of steepest descent followed by 1000 of conjugate gradient of the entire system.

The molecular dynamics simulations were performed using periodic boundary conditions. The previously minimized systems were initially equilibrated at 300K for 50 ps in a canonical ensemble, using Langevin dynamics. Production simulations were carried at 300K using Langevin dynamics with a collision frequency of 1.0 ps^{-1}. Constant pressure periodic boundary was used with an average pressure of 1 atm. Isotropic position scaling was used to maintain the pressure with a relaxation time of 2 ps. The time step was set to 2 fs. Shake constraints were applied to all bonds involving hydrogen atoms. The particle mesh Ewald (PME) method was used to calculate the electrostatic interactions. All intermolecular interactions were treated with a cut-off distance of 12 Å. The trajectories were saved every 100 steps for analysis. The length of the production run was 1112 ps.

ACKNOWLEDGEMENTS

We thank the financial support from Fundação para a Ciência e a Tecnologia (Portugal) for the fellowship SFRH/BD/17845/2004, and the National Foundation for Cancer Research (NFCR, USA).

REFERENCES

[1] Telesnitsky, A.; Goff, S.P. In *Retroviruses;* Coffin, J.M.; Hughes S.H.; And Varmus, H.E., Ed., Cold Spring Harbor Laboratory Press, Cold Spring Harbor, NY, **1997**.

[2] Mizrahi V.; Lazarus G.M.; Miles L.M.; Meyers C.A.; Debouck C. *Arch. Biochem. Biophys*., **1989**, *273*(2), 347.

[3] Kohlstaedt L.A.; Wang J.; Friedman J.M.; Rice P.A.; Steitz T.A. *Science*, **1992**, *256*(5065), 1783.

[4] Le Grice S.F.; Naas T.; Wohlgensinger B.; Schatz O. *EMBO J*., **1991**, *10*(12), 3905.

[5] Johnson, M.S.; McClure, M.A.; Feng, D.F.; Gray, J.; Doolitle, R.F. *Proc. Natl. Acad. Sci. USA*, **1986**, *83*, 7648.

[6] Larder, B.A.; Purifoy, D.J.M.; Powell, K.L.; Darby, G. *Nature*, **1987**, *327*, 716.

[7] Majumdar, C.; Abbotts, J.; Broder, S.; Wilson, S. *J. Biol. Chem*., **1988**, *263*(30),15657.

[8] Wöhrl, B.M.; Krebs, R.; Goody, R.S.; Restle, T. *J. Mol. Biol*., **1999**, 333.

[9] Unge, T.; Knight, S.; Bhikhabhai, R.; Lovgren, S.; Dauter, Z.; Wilson, K.; Strandberg, B. *Structure*, **1994**, *2,* 953.
[10] Rodgers, D.W.; Gamblin, S.J.; Harris, B.A.; Ray, S.; Culp, J.S.; Hellmig, B.; Woolf, D.J.; Debouck, C.; Harrison, S.C. *Proc. Natl. Acad. Sci .USA*, **1995**, *2,* 1222.
[11] Esnouf, R.; Ren, J.; Ross, C.; Jones, Y.; Stammers, D.; Stuart, D. *Nat. Struct .Biol*., **1995**, *2*, 303.
[12] Hsiou, Y.; Ding, J.; Das, K.; Clark Jr. A.D.; Hughes, S.H.; Arnold, E. *Structure*. **1996**, *4*, 853.
[13] Hsiou, Y.; Ding, J.; Das, K.; Clark Jr. A.D.; Boyer, P.L.; Lewi, P.; Janssen, P.A.; Kleim, J.P.; Rosner, M.; Hughes, S.H.; Arnold, E. *J. Mol .Biol*., **2001**, *309*, 437.
[14] Sarafianos, S.G.; Das, K.; Clark Jr. A.D.; Ding, J.; Boyer, P.L.; Hughes, S.H.; Arnold, E. *Proc. Natl. Acad. Sci. USA*, **1999**, *96*, 10027.
[15] Ren, J; Nichols, C.; Bird, L.; Chamberlain, P.; Weaver, K.; Short, S.; Stuart, D.I.; Stammers, D.K. *J. Mol. Biol*. **2001**, *312*, 795.
[16] Ding, J.; Das, K.; Hsiou, Y.; Sarafianos, S.G.; Clark, A.D. Jr.; Jacobo-Molina, A.; Tantillo, C.; Hughes, S.H.; Arnold, E. . *J. Mol. Biol*., **1998**, *284*, 1095.
[17] Sarafianos, S.G.; Das, K.; Tantillo, C.; Clark Jr. A.D.; Ding, J.; Whitcomb, J.M.; Boyer, P.L.; Hughes, S.H.; Arnold, E. . *EMBO J*., **2001**, *20*, 1449.
[18] Peletskaya, E.N.; Kogon, A.A.; Tuske, S.; Arnold, E.; Hughes, S.H. *J. Virol*., **2004**, *78*, 3387.
[19] Huang, H.; Chopra, R.; Verdine, G.L.; Harrison, S.C. *Science*, **1998**, *282*, 1669.
[20] Sarafianos, S.G. *et al*. *EMBO J*. **2002**, *21*, 6614.
[21] Tuske S.; Sarafianos S.G.; Clark A.D. Jr.; Ding J.; Naeger L.K.; White K.L.; Miller M.D.; Gibbs C.S.; Boyer P.L.; Clark P.; Wang G.; Gaffney B.L.; Jones R.A.; Jerina D.M.; Hughes S.H.; Arnold E. *Nat Struct Mol Biol.,* **2004**, *11*(5), 469.
[22] Wang, J.; Smerdon, S.J. ; Jager, J. ; Kohlstaedt, L.A. ; Rice, P.A. ; Friedman, J.M. ; Steitz, T.A. *Proc. Natl. Acad. Sci. USA*. **1994**, *91*, 7242.
[23] Ding, J.; Das, K.; Tantillo, C.; Zhang, W.; Clark Jr. A.D.; Jessen, S.; Lu, X.; Hsiou, Y.; Jacobo-Molina, A.; Andries, K. et al. *Structure,* **1995**, *3*, 365.
[24] Ding, J.; Das, K.; Moereels, H.; Koymans, L.; Andries, K.; Janssen, P.A.; Hughes, S.H.; Arnold, E. *Nat. Struct. Biol*. **1995**, *2,* 407.
[25] Ren, J.; Esnouf, R.; Hopkins, A.; Ross, C.; Jones, Y.; Stammers, D.; Stuart, D. *Structure*, **1995**, *3*, 915.
[26] Ren, J.; Esnouf, R.; Garman, E.; Somers, D.; Ross, C.; Kirby, I.; Keeling, J.; Darby, G.; Jones, Y.; Stuart, D. *et al*. *Nat. Struct. Biol*., **1995**, *2*, 293.
[27] Ren, J.; Esnouf, R.M.; Hopkins, A.L.; Jones, E.Y.; Kirby, I.; Keeling, J.; Ross, C.K.; Larder, B.A.; Stuart, D.I.; Stammers, D.K. *Proc. Natl. Acad. Sci. USA*, **1998**, *95*, 9518.
[28] Ren, J.; Esnouf, R.M.; Hopkins, A.L.; Warren, J.; Balzarini, J.; Stuart, D.I.; Stammers, D.K. *Biochemistry*, **1998**, *37,* 14394.
[29] Ren, J.; Esnouf, R.M.; Hopkins, A.L.; Stuart, D.I.; Stammers, D.K. *J. Med. Chem*., **1999**, *42*, 3845.
[30] Ren, J.; Diprose, J.; Warren, J.; Esnouf, R.M.; Bird, L.E.; Ikemizu, S.; Slater, M.; Milton, J.; Balzarini, J.; Stuart, D.I.; Stammers, D.K. *J. Biol. Chem*., **2000**, *275*, 5633.
[31] Ren, J.; Nichols, C.; Bird, L.E.; Fujiwara, T.; Sugimoto, H.; Stuart, D.I.; Stammers, D.K. *J. Biol. Chem*., **2000**, *275,* 14316.
[32] Ren, J.; Milton, J.; Weaver, K.L.; Short, S.A.; Stuart, D.I.; Stammers, D.K. *STRUCTURE FOLD. DES*., **2000**, *8*, 1089.
[33] Ren, J.; Nichols, C.E.; Chamberlain, P.P.; Weaver, K.L.; Short, S.A.; Stammers, D.K. *J. Mol. Biol.,* **2004**, *336*, 569.
[34] Hopkins, A.L.; Ren, J.; Esnouf, R.M.; Willcox, B.E.; Jones, E.Y.; Ross, C.; Miyasaka, T.; Walker, R.T.; Tanaka, H.; Stammers, D.K.; Stuart, D.I. *J. Med. Chem*., **1996**, *39*, 1589.
[35] Hopkins, A.L.; Ren, J.; Tanaka, H.; Baba, M.; Okamato, M.; Stuart, D.I.; Stammers, D.K. *J. Med. Chem.* **1999**, *42*, 4500.
[36] Das, K.; Ding, J.; Hsiou, Y.; Clark Jr., A.D.; Moereels, H.; Koymans, L.; Andries, K.; Pauwels, R.; Janssen, P.A.; Boyer, P.L.; Clark, P.; Smith Jr., R.H.; Kroeger, M.B.; Michejda, C.J.; Hughes, S.H.; Arnold, E. *J. Mol. Biol.,* **1996**, *264*, 1085.
[37] Das, K.; Clark Jr., A.D.; Lewi, P.; Heeres, J.; Dejonge, M.; Koymans, L.; Vinkers, H.; Daeyaert, F.; Ludovici, D.W.; Kukla, M.J.; Decorte, B.; Kavash, R.W.; Ho, C.Y.; Ye, H.; Lichtenstein, M.; Andries, K.; Pauwles, R.; Debethune, M.-P.; Boyer, P.L.; Clark, P.; Hughes, S.H.; Janssen, P.A.; Arnold, E. *J. Med. Chem*., **2004**, *47*, 2550.
[38] Esnouf, R.M.; Ren, J.; Hopkins, A.L.; Ross, C.K.; Jones, E.Y.; Stammers, D.K.; Stuart, D.I. *Proc. Natl. Acad. Sci*. USA, **1997**, *94*, 3984.
[39] Hsiou, Y.; Das, K.; Ding, J.; Clark Jr., A.D.; Kleim, J.P.; Rosner, M.; Winkler, I.; Riess, G.; Hughes, S.H.; Arnold, E. *J. Mol. Biol*., **1998**, *284*, 313.
[40] Hogberg, M.; Sahlberg, C.; Engelhardt, P.; Noreen, R.; Kangasmetsa, J.; Johansson, N.G.; Oberg, B.; Vrang, L.; Zhang, H.; Sahlberg, B.L.; Unge, T.; Lovgren, S.; Fridborg, K.; Backbro, K. *J. Med. Chem.,* **2000**, *43*, 304.
[41] Chan, J.H.; Hong, J.S.; Hunter 3rd., R.N.; Orr, G.F.; Cowan, J.R.; Sherman, D.B.; Sparks, S.M.; Reitter, B.E.; Andrews 3rd., C.W.; Hazen, R.J.; St Clair, M.; Boone, L.R.; Ferris, R.G.; Creech, K.L.; Roberts, G.B.; Short, S.A.; Weaver, K.; Ott, R.J.; Ren, J.; Hopkins, A.; Stuart, D.I.; Stammers, D.K. *J. Med. Chem*., **2001**, *44*, 1866.
[42] Lindberg, J.; Sigurdsson, S.; Lowgren, S.; Andersson, H.O.; Sahlberg, C.; Noreen, R.; Fridborg, K.; Zhang, H.; Unge, T. *Eur. J. Biochem*., **2002**, *269*, 1670.
[43] Pata, J.D.; Stirtan, W.G.; Goldstein, S.W.; Steitz, T.A. *Proc. Nat. Acad. Sci. USA,* **2004**, *101*, 10548.
[44] Sarafianos, S.G.; Das, K.; Tantillo, C.; Clark Jr., A.D.; Ding, J.; Whitcomb, J.M.; Boyer, P.L.; Hughes, S.H.; Arnold, E. *EMBO J*., **2001**, *20*, 1449.
[45] Kensch, O.; Restle, T.; Wöhrl, B.M.; Goody, R.S.; Steinhoff, H.-J. *J. Mol. Biol*., **2000**, *301*, 1029.
[46] Guex, N..; Peitsch, M.C. *Electrophoresis*, **1997**, *18*, 2174.
[47] G.Vriend. *J. Mol. Graph*., **1990**, *8,* 52.
[48] Case, D.A.; Darden, T.A.; Cheatham, T.E.; Simmerling, III, C.L.; Wang, J.; Duke, R.E.; Luo, R.; Merz, K.M.; Wang, B.; Pearlman, D.A.; Crowley, M.; Brozell, S.; Tsui, V.; Gohlke, H.; Mongan, J.; Hornak,V.; Cui, G.; Beroza, P.; Schafmeiste,r C.; Caldwell, J.W.; Ross, W.S.; Kollman, P.A. AMBER 8, **2004**, University of California, San Francisco.
[49] Cornell, W.D.; Cieplak P.; Bayly C.I.; Gould I.R.; Merz K.M. Jr.; Ferguson D.M.; Spellmeyer D.C.; Fox T.; Caldwell J.W.; Kollman P.A. *J.A. Chem. Soc*., **1995**. *117*, 5179.

Received: 09 March, 2006 **Revised: 14 June, 2006** **Accepted: 19 June, 2006**